Eur Biophys J (1996) 24: 137–141

European Biophysics Journal

Orientational steering in enzyme-substrate association: Ionic strength dependence of hydrodynamic torque effects

Jan Antosiewicz[1,2,*], **James M. Briggs**[1,2], **J. Andrew McCammon**[1,2]

[1] Department of Chemistry and Biochemistry, University of California at San Diego, La Jolla, CA 92093-0365, USA
[2] Department of Pharmacology, University of California at San Diego, La Jolla, CA 92093-0365, USA

Received: 8 September 1995/ Accepted in revised form: 24 November 1995

Abstract. The effect of hydrodynamic torques on the association rate constants for enzyme-ligand complexation is investigated by Brownian dynamics simulations. Our hydrodynamic models of the enzyme and ligand are composed of spherical elements with friction forces acting at their centers. A quantitative measure of hydrodynamic torque orientational effects is introduced by choosing, as a reference system, an enzyme-ligand model with the same average hydrodynamic interactions but without orientational dependence. Our simple models show a 15% increase in the rate constant caused by hydrodynamic torques at physiological ionic strength. For more realistic hydrodynamic models, which are not computationally feasible at present, this effect is probably higher. The most important finding of this work is that hydrodynamic complementarity in shape (i.e. like the fitting together of pieces of a puzzle) is most effective for interactions between molecules at physiological ionic strength.

Key words: Hydrodynamic torques - Enzyme-substrate association - Ionic strength dependence

1. Introduction

The first step in many biological processes is the diffusional encounter of ligand and receptor molecules (McCammon and Harvey 1987). The importance of two long-range interactions in the encounter processes has been recognized for a long time. These are electrostatic interactions, see e.g. (Head-Gordon and Brooks 1987; Northrup et al. 1987) and hydrodynamic interactions, see e.g. (Allison et al. 1984; Northrup et al. 1984). An interesting aspect of such encounters arises in situations where the molecules not only must be brought into close proximity, but also must be oriented correctly in space for a successful encounter (e.g. binding or reaction) to occur. The role of electrostatic torques in speeding certain enzymatic reactions has been demonstrated (Luty et al. 1993; Wade et al. 1994). More recently, Brune and Kim (1994) have suggested that in the case of a cleft enzyme interacting with an elongated substrate, hydrodynamic steering torques could also play a significant role. Our recent Brownian dynamics simulations (Antosiewicz and McCammon 1995) for enzyme-substrate systems, with hydrodynamic and electrostatic torques favoring two different orientations of the mutually approaching enzyme and substrate, showed that the hydrodynamic torque effect is not dominant over the electrostatic torque effect. We suggested that somewhat larger effects due to hydrodynamic torques could occur in cases where hydrodynamic interactions (HI) and electrostatic interactions (EI) favor the same orientation, or when stronger attraction due to EI leads to larger velocities of approach. These possibilities are studied in the present work.

Our preliminary simulations indicated that simply neglecting HI does not provide good reference models for studying the effect of hydrodynamic torques. Therefore, we developed a method for extracting orentational effects from overall hydrodynamic effects by designing a reference model with the same orientationally-averaged HI but without HI torques.

It is shown that for our simple models of the enzyme and substrate, the maximal effect of hydrodynamic torques results in a 15% increase in the diffusional encounter rate constant in comparison to the reference models where the overall hydrodynamic forces are the same but torques due to these forces are absent. This is not a large effect, but this may be due in part to our use of a bead model approach with relatively few beads to model the shape of particles. It is probable that hydrodynamic models referring hydrodynamic forces to the surfaces of particles described by triangulation methods (Brune and Kim 1994) would give a larger increase. However, an interesting result of our study is that the relative increase in the rate constant is close to zero at zero ionic strength, and rises to a maximum when the ionic strength approaches 150 mM. This suggests that enzymes make the best use of combined electrostatic and hydrodynamic interactions around physiological ionic strength.

* *Current address*: Department of Biophysics, University of Warsaw, PL-02-089 Warsaw, Poland
Correspondence to: J.M. Briggs

2. Methods

2.1. Theoretical basis

The hydrodynamic part of our calculation is based on spherical bead models of molecules with hydrodynamic forces acting at the centers of the beads, see e.g. Ermak and McCammon (1978), Garcia de la Torre and Bloomfield (1981). The electrostatic part of the calculation is based on the finite-difference Poisson-Boltzmann method for the calculation of the electrostatic potential around the enzyme model (Warwicker and Watson 1982, Davis and McCammon 1990, Sharp and Honig 1990, Madura et al. 1994, Sharp 1994). Brownian dynamics calculations are based on the algorithm described by Ermak and McCammon (1978) as implemented in the UHBD software (Davis et al. 1991; Madura et al. 1994).

A detailed description of the methods used in this work is presented elsewhere (Antosiewicz and McCammon 1995), and only modifications and the basic points of this description are included below.

2.2. Software

The Brownian dynamics simulations described in this work are done using the UHBD program (Davis et al. 1991, Madura et al. 1994). Modifications to the program were described in the previous work (Antosiewicz and McCammon 1995). The version used for the present work differs from the previous one in that rotations of the enzyme are introduced. Thus the algorithm consists of the following steps.

1. All beads move according to stochastic and electrostatic forces.
2. The positions of all beads are corrected for displacement of the center of mass of the enzyme.
3. Corrected coordinates of the enzyme beads are used to find the rotation of the enzyme relative to the situation before the Brownian step was taken.
4. The rotation determined in the previous step is used to correct positions of the substrate beads, while the coordinates of the enzyme's beads finally remain effectively unchanged.

The third point in the above list requires a more detailed description. When the coordinates of all beads are corrected for displacement of the center of mass of the enzyme, then the center of mass of the enzyme before and after the Brownian step coincide. Let $\mathbf{u}_i$ be a unit vector at the center of the enzyme pointing toward its first subunit before the step and $\mathbf{u}_f$ be the analogous vector after a Brownian step and translational correction. The vector product of these two unit vectors gives a vector whose direction is that of the rotation axis and whose length is the sinus of the angle of rotation. An opposite rotation around this axis is applied to all substrate beads, thereby leaving the coordinates of the enzyme's beads unchanged for the next Brownian step. When the center of the enzyme is initially at the origin of the coordinate system, the coordinates of each of the substrate's subunits are found from the equation:

$$\mathbf{r}_{substrate,f} = \mathbf{r}_{substrate,i}\cos\alpha + \mathbf{v}\times\mathbf{r}_{substrate,i}\sin\alpha + (1-\cos\alpha)\mathbf{v}(\mathbf{v}\cdot\mathbf{r}_{substrate,i})$$

where $\mathbf{v}$ is the unit vector along the rotation axis. When the center of the enzyme has an initial position $\mathbf{r}_c$, as the first step the coordinates of the substrate should be translated by the vector $-\mathbf{r}_c$, and after rotation is done according to the above equation, they should be translated by the rotated vector $\mathbf{r}_c$.

2.3. Models

2.3.1. Models of the enzyme. There are three different aspects of the modeling of our enzyme: hydrodynamic interaction centers, charge distribution and low dielectric area, and substrate non-accessible volume. Two different enzyme models for the hydrodynamic interactions are considered along with two different electric models (i.e. charged and uncharged). In all cases, the excluded volume aspects are the same (as described below). Hydrodynamic and excluded volume aspects of the models of the enzyme and substrate are illustrated in Fig. 1.

Our simple hydrodynamic model of a cleft enzyme consists of two spheres. Each is treated as a point source of friction located at the center of each bead, having hydrodynamic interactions with the second bead (Garcia de la Torre and Bloomfield 1981). As a reference model for studying the effects of HI torques in the encounter of our enzyme with a dumbbell model of the substrate, a single-sphere hydrodynamic model of the enzyme is also considered (i.e. a hydrodynamic monomer model). The radius of this sphere is such that the average translational diffusion coefficients of the hydrodynamic dumbbell model and the hydrodynamic monomer model are the same. We do not want to have the hydrodynamic radius of the single sphere be larger than 20.0 Å; thus we arrive at 13.3 Å as the radii of the spheres of the dumbbell model (with centers separated by 40 Å) and a radius of the single sphere model which is 20.07 Å.

Regarding substrate exclusion properties, the enzyme consists of 3 "atoms". Each sphere is 20 Å in radius, separated by 20 Å along a straight line, and defines the volume not available for the beads of the substrate. Note that this same model for the exclusion properties was used for all calculations even though it's hydrodynamic properties were modeled either by a single sphere or two spheres as described above.

Finally, the electric properties are such that the terminal 20 Å spheres are uncharged and the central 20 Å bead has a charge of +10e. The second electric case considered was for all charges set to zero.

2.3.2. Models of the substrate. The substrate is modeled as two 5 Å spheres separated by 11 Å. These two spheres define the hydrodynamic properties of the substrate and volume occupied by it. Regarding electric properties of the model, each of the beads has a charge of –2e. Charges of the substrate are treated as point test charges which do not disturb the field created by the enzyme. This means that the radii of the substrate beads are effectively added to the Debye screening by the solvent with a non-zero ionic strength.

2.3.3. Relative diffusion coefficient of substrate. The relative diffusion coefficients between the enzyme and ligand for the hydrodynamic monomer–dumbbell and hydrodynamic dumbbell–dumbbell arrangements were calculated by a simple program based on an algorithm for Brownian motion of spherical beads where hydrodynamic interactions between them have been included (Ermak and McCammon 1978). A monomeric or dumbbell model of the enzyme was put in the center of the coordinate system and the model of the ligand was put randomly on a sphere of radius R with a randomly chosen orientation with respect to the enzyme. Subsequently all HI beads (i.e. 3 in the first case or 4 in the second case) were allowed to make a predefined number of Brownian steps. For each step the relative diffusion coefficient of the ligand with respect to the enzyme along the i-th axis was calculated from the relation:

$$D_i = \Delta x_i \Delta x_i / 2\Delta t \tag{1}$$

Δx_i is the relative displacement along the i-th axis during time interval Δt. The quantities D_i were averaged over positions and orientations of the sphere of radius R and the number of steps taken for each sampled position and orientation. The average relative translational diffusion coefficient was taken as one third of $D_1 + D_2 + D_3$.

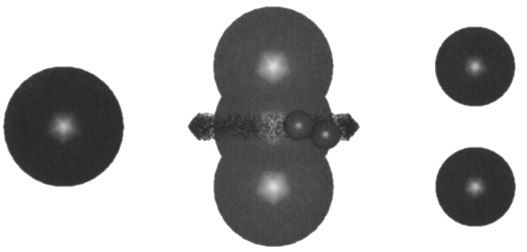

Fig. 1. Schematic representation of the models of a cleft enzyme and an elongated ligand used in the present work. The central part shows the volume unavailable for our dumbbell substrate built of two 5 Å spheres with centers separated by 11Å. A randomly selected orientation of the substrate with respect to the enzyme, which satisfies the reaction criteria is shown as an example. A dotted ring shows the volume available for the center of the substrate beads for which the reaction criteria are satisfied. The left part shows the monomeric hydrodynamic model of the enzyme and the right part shows the dimeric hydrodynamic model, equivalent to the monomeric with respect to the average translational diffusion coefficient

2.4. Criteria for diffusional encounter

Diffusional encounter is considered to be completed when both beads of the substrate are located within 35 Å from each of the enzyme's three "atoms". This condition can be satisfied when the coordinates of the beads of the substrate are within a dotted ring volume shown in Fig. 1. From this figure it can be seen that this corresponds to a fairly clear perpendicular orientation of the axes of the enzyme and the substrate. The figure also shows one possible orientation of the beads of the substrate satisfying the encounter criteria.

2.5. Summary of the Brownian dynamics simulation method

The bimolecular rate constant, k, for diffusional encounter between an enzyme and its ligand can be represented as (Madura et al. 1994)

$$k = k(b) \cdot \beta \tag{2}$$

where $k(b)$ is the rate at which the ligand initially reaches a spherical surface of radius b centered on the enzyme, and β is, in effect, the probability that the ligand, having encountered this "b-surface", will proceed to encounter the active site rather than wandering away to infinity. If b is chosen large enough that the potential of mean force U between the reactants is centrosymmetric for distances larger than b, then $k(b)$ can be found by solving the one-dimensional diffusion equation, leading to

$$k(b)^{-1} = \int_b^\infty \frac{e^{U(r)/k_B T}}{4\pi D r^2} \mathrm{d}r \tag{3}$$

where $k_B T$ is Boltzmann's constant multiplied by temperature, and D is the relative diffusion coefficient. The quantity β is the probablity that a ligand started at a random location on the "b surface" will reach the active site of the enzyme. This probability is estimated by the generation of a large number of Brownian dynamics trajectories of the ligand around the enzyme and then finding the fraction of trajectories that end with encounter (Madura et al. 1994). All Brownian dynamics trajectories are started at randomly chosen positions on the sphere of radius b, and are terminated after successful encounter with the enzyme, or when they reach the surface of a "quit" sphere with radius $q > b$. There is another sphere used during simulations, namely a sphere of radius $p < b$. When the ligand is inside the p sphere, the reaction criteria are checked after each Brownian dynamics step.

2.6. Technical details of the simulations

For cases considered here, 20000 Brownian dynamics trajectories were generated using 60×60×60 cubic grids with a grid point spacing 2.0 Å. The radius of the b sphere was 60.0 Å, that of the p sphere was 55.0 Å, and the radius of the q sphere was 120.0 Å.

A variable time step was used. The time step was 0.4 ps within a 52 Å sphere defined by the center of the enzyme, between 52 and 60 Å it was 4.0 ps, between 60 and 80 Å it was 20 ps, and for distances larger than 80 Å it was 100 ps. These time intervals lead to spatial steps of the order of a fraction of an Angstrom inside the p sphere.

The modified Oseen hydrodynamic interaction tensor was used with stick boundary conditions (Oseen 1927; Garcia de la Torre and Bloomfield 1981). Overlapping between beads of the enzyme and the substrate was not allowed.

A temperature of 300 K was used and ionic strengths in the range of 0 to 300 mM were considered. The solvent

Table 1. Relative diffusion coefficients D for the dumbbell substrate, as a function of radial distance between centers of the enzyme and substrate, for the dumbbell model of the enzyme, and the single sphere model of the enzyme with the same translational diffusion coefficient as the dumbbell. The 95% confidence limit error in the calculated values is below $0.05 \times 10^{-6} \mathrm{cm}^2\mathrm{s}^{-1}$

r (Å)	$D_{dumbbell,sphere}$ ($10^{-6}\mathrm{cm}^2\mathrm{s}^{-1}$)	$D_{dumbbell,dumbbell}$ ($10^{-6}\mathrm{cm}^2\mathrm{s}^{-1}$)
1000	4.78	4.77
500	4.73	4.72
250	4.63	4.62
120	4.42	4.41
60	4.01	3.99
44	3.72	3.70

dielectric constant was set to 78 and the enzyme's dielectric constant was set to 2.

3. Results and discussion

3.1. Relative diffusion coefficients

The hydrodynamic monomer and hydrodynamic dumbbell models of the enzyme are equivalent in the sense that their average translational diffusion coefficient is the same. The model of the ligand is always the same, i.e. a hydrodynamic dumbbell.

Table 1 shows the relative diffusion coefficients for the enzyme-ligand systems for the two models of the enzyme. It can be seen that down to a distance of 44 Å between the centers of the enzyme and substrate, both models give the same relative diffusion coefficient of the substrate. Thus, it was expected that a comparison between rate constants for both models of the enzyme would provide a good measure for hydrodynamic interaction orientational effects for enzyme-substrate encounters.

3.2. Contribution of hydrodynamic orientational steering to the rate constants of diffusional encounter

Results from the Brownian dynamics simulations are presented as the relative increase in the diffusional rate constant $\Delta = \frac{(k_{d,d} - k_{s,d})}{k_{s,d}}$ as a function of ionic strength I ($k_{d,d}$ stands for $k_{dumbbell,dumbbell}$ and $k_{s,d}$ stands for $k_{sphere,dumbbell}$). These results are shown in Fig. 2. The error bars are calculated according to the following equation:

$$\delta\Delta = \sqrt{\frac{(\delta k_{d,d})^2}{k_{s,d}^2} + \frac{k_{d,d}^2 (\delta k_{s,d})^2}{k_{s,d}^4}} \tag{4}$$

Errors for individual rate constants ($\delta k_{d,d}$ and $\delta k_{s,d}$) correspond to 90% confidence errors provided by the UHBD program, therefore the error bars for Δ also correspond to this confidence level.

Although the overall effect of hydrodynamic orientational torques is not large (15% and below) it seems very interesting that it decreases with decreasing ionic strength (i.e. when electrostatic interactions become larger).

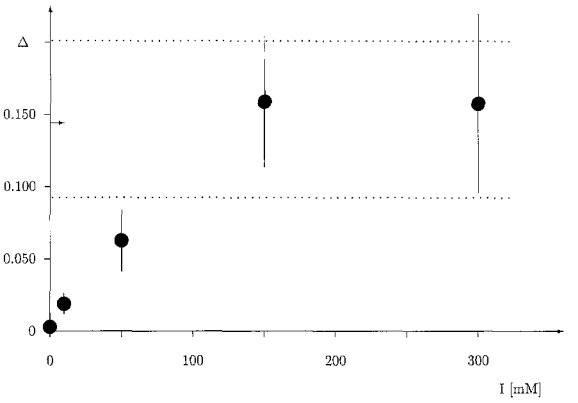

Fig. 2. Relative increase in the diffusional rate constant $\Delta = \frac{(k_{dumbbell,dumbbell} - k_{sphere,dumbbell})}{k_{sphere,dumbbell}}$ as a function of ionic strength I. The horizontal arrow on the perpendicular axis indicates the average value of Δ for non-charged particles with the same hydrodynamic properties, and the horizontal dotted lines indicate the estimated error range for the non-charged case

Calculations for neutral models of the enzyme and the ligand were also performed and the observed effects were very small, i.e., in the whole range of ionic strengths the increase in the rate was around 15%, with very slight drop for zero ionic strength. More accurate results would require significantly larger number of simulated trajectories which currently prohibits their undertaking.

It seems that the result with the charged model of enzyme and ligand is more meaningful for biological systems as the enzymes are frequently charged at physiological pH, and even if not, they usually have charged parts distributed over their structure, so locally (e.g. for small distances between the substrate and the active site) they interact like charged species.

3.3. Conclusions

Although the hydrodynamic torque orientational steering effects computed in the present work are rather small, which confirms the results of our previous work (Antosiewicz and McCammon 1995), it seems that there are two new noteworthy aspects.

The first is that our method to extract the influence of hydrodynamic interaction torques on the diffusional encounter from the overall hydrodynamic interactions appears to be useful as a quantitative measure of the effect.

The second is that the ionic strength dependence of the relative increase in the diffusional encounter rate constant due to hydrodynamic torques has interesting biological implications.

The calculated effect is small which is partly a result of a weakness in our bead model approach to hydrodynamics. With only two spheres for each model, with frictional forces acting in the centers of the beads, hydrodynamic interactions are underestimated. Using a larger number of smallerbeads

to model the surface of a cleft enzyme would probably give larger effects but is not computationally feasible at present. On the other hand, the approach to the hydrodynamic problem where friction forces act at surface elements of the models, as done by Brune and Kim (1994), which is expected to give larger effects due to hydrodynamic torques, is not implemented in the UHBD program. But it is likely that the ionic strength dependence shown in Fig. 2 will be similar when using a larger number of beads or a surface element approach.

The decrease in Δ shown in Fig. 2 when the ionic strength decreases means that complementarity in shape between a cleft enzyme and an elongated substrate cannot be effectively used to discriminate hydrodynamically among substrates of different shapes when electrostatic forces are too strong. Many enzymes are charged at physiological pH values, or even if they have a total charge of zero, they have separate charged subdomains leading to strong electrostatic interactions for close distances between an enzyme's surface and the ligand. It seems that an ionic strength of 150 mM is well suited to attenuate electrostatic interactions in such a way that the hydrodynamic utility of shape complementarity is the greatest. Physically, the probable reason that Δ decreases at low ionic strength is that the stronger electrostatic attraction holds the encounter complex together for longer times, allowing the orientational criteria to be satisfied.

It is also worth noting that the 15% increase in the rate constant caused by the hydrodynamic torque effect, observed in the present work, can be interpreted in the following way. Our previous work (Antosiewicz and McCammon 1995) indicated a 15-20% decrease in the calculated rate constant when hydrodynamic interactions were introduced into Brownian dynamics simulations. This result was obtained with the same bead model approach used in the present work. Therefore we can say that the existence of hydrodynamic torques results in returning the rate constants to the range of values obtained with simulations in which hydrodynamic interactions are not included. It is probable that a qualitatively similar picture will be obtained with a more sophisticated approach to the calculation of hydrodynamic interactions.

Acknowledgement. This work was supported in part by grants from NIH and the NSF supercomputer centers MetaCenter program.

References

Allison SA, Srinivasan N, McCammon JA, Northrup SH (1984) Diffusion-controlled reactions between a spherical target and dumbell dimer by brownian dynamics simulation. J Phys Chem 88:6152–6157

Antosiewicz J, McCammon JA (1995) Electrostatic and hydrodynamic orientational steering effects in enzyme-substrate association. Biophys J 69:57–65

Brune D, Kim S (1994) Hydrodynamic steering effects in protein association. Proc Natl Acad Sci USA 91:2930–2934

Davis ME, McCammon JA (1990) Electrostatics in biomolecular structure and dynamics. Chem Rev 90:509–521

Davis ME, Madura JD, Luty BA, McCammon JA (1991) Electrostatics and diffusion of molecules in solution: simulations with the University of Houston Brownian Dynamics program. Comp Phys Commun 62:187–197

Ermak DL, McCammon JA (1978) Brownian dynamics with hydrodynamic interactions. J Chem Phys 69:1352–1360

Garcia de la Torre J, Bloomfield VA (1981) Hydrodynamic properties of complex, rigid, biological macromolecules: theory and applications. Q Rev Biophys 14:81–139

Head-Gordon T, Brooks CL (1987) The role of electrostatics in the binding of small ligands to enzymes. J Phys Chem 91:3342–3349

Luty BA, Wade RC, Madura JD, Davis ME, Briggs JM, McCammon JA (1993) Brownian dynamics simulations of diffusional encounters between triose phosphate isomerase and glyceraldehyde phosphate: Electrostatic steering of glyceraldehyde phosphate. J Phys Chem 97:233–237

Madura JD, Gilson, MEDMK, Wade RC, Luty BA, McCammon JA (1994) Biological applications of electrostatic calculations and brownian dynamics simulations. Rev Comput Chem 5:229–267

McCammon JA, Harvey SC (1987) Dynamics of proteins and nucleic acids. Cambridge Univ. Press, Cambridge

Northrup SH, Allison SA, McCammon JA (1984) Brownian dynamics simulation of diffusion-influence bimolecular reactions. J Chem Phys 80:1517–1524

Northrup SH, Boles JO, Reynolds JCL (1987) Electrostatic effects in the brownian dynamics of association and orientation of heme proteins. J Phys Chem 91:5991–5998

Oseen CW (1927) Neuere Methoden und Ergebnisse in der Hydrodynamik. Akademische Verlagsgesellschaft M B H, Leipzig

Sharp KA (1994) Electrostatic interactions in macromolecules. Curr Opinion Struct Biol 4:234–239

Sharp KA, Honig B (1990) Electrostatic interactions in macromolecules. Theory and applications. Annu Rev Biophys Chem 19:301–332

Wade RC, Luty BA, Demchuk E, Madura JD, Davis ME, Briggs JM, McCammon JA (1994) Simulation of enzyme-substrate encounter with gated active sites. Nature Struct Biol 1:65–69

Warwicker J, Watson HC (1982) Calculation of the electric potential in the active site cleft due to α-helix dipoles. J Mol Biol 157:671–679